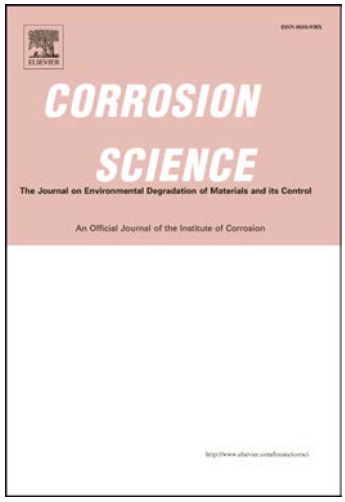

Oxidation and corrosion protection by halide treatment of powder metallurgy Ti and Ti6Al4V alloy

S.A. Tsipas, E. Gordo, A. Jiménez-Morales

PII: S0010-938X(14)00353-9
DOI: http://dx.doi.org/10.1016/j.corsci.2014.07.037
Reference: CS 5958

To appear in: *Corrosion Science*

Received Date: 10 April 2014
Accepted Date: 16 July 2014

Please cite this article as: S.A. Tsipas, E. Gordo, A. Jiménez-Morales, Oxidation and corrosion protection by halide treatment of powder metallurgy Ti and Ti6Al4V alloy, *Corrosion Science* (2014), doi: http://dx.doi.org/10.1016/j.corsci.2014.07.037

Oxidation and corrosion protection by halide treatment of powder metallurgy Ti and Ti6Al4V alloy

S.A. Tsipas[a*], E. Gordo[a], A. Jiménez-Morales[a]

[a]Departamento de Ciencia e Ingeniería de Materiales e Ingeniería Química, IAAB, Universidad Carlos III de Madrid, Avda. de la Universidad, 30, 28911 Leganés, Madrid, stsipas@ing.uc3m.es; egordo@ing.uc3m.es ; toni@ing.uc3m.es

*Corresponding author stsipas@ing.uc3m.es, Tel.+34916248374, Fax: +34916249430

Abstract

The aim of this work is to study the effect of halide treatment in powder metallurgy Ti-6Al-4V alloy, in order to improve high temperature oxidation and electrochemical corrosion resistance. Halide treatment was performed by immersing samples in a powder mixture containing 3 wt% NH_4Cl, at 200°C and 950°C. Oxidation resistance was assessed by exposure to 600°C for 300 hours. The microstructure and phase constitution of the formed oxide layers was characterized. Corrosion resistance in aircraft simulated environment was evaluated with Electrochemical Impedance Spectroscopy. Notable improvement in oxidation and corrosion resistance was observed for samples treated at 200°C.

Keywords: titanium A; EIS B, thermodynamic diagrams C; atmospheric corrosion C; selective oxidation C; oxide coatings C.

Introduction

Titanium alloys are widely used for their excellent mechanical properties and relatively low density. However, in some applications, such as those required in aeronautics or in biomedical engineering, alloys are required to meet much more demanding specifications in order to improve their performance not only in wet environments but also at high temperatures. For this reason, there is growing interest directed towards finding new surface treatments that confer to titanium alloys increased resistance to aqueous corrosion, aircraft-simulated environment and oxidation at high temperature in extreme service conditions to which they will subjected in these sectors while maintaining their mechanical properties[1-7].

In this context, it has been observed that the addition of small amounts of halogen elements into the surface of certain intermetallic Ti-Al alloys produced a significant

improvement in their oxidation resistance [8, 9]. The small amounts of halogen introduced into the surface of the metal cause the formation of gaseous aluminium halides which oxidize and activate a mechanism of selective oxidation of aluminium. The kinetics change from fast oxidation kinetics that cause the formation of a mixed oxide layer of TiO_2 and Al_2O_3 to slow oxidation kinetics in which only the aluminium is oxidized [9-11]. The oxide layer formed contains only Al_2O_3 which is more protective against further oxidation reactions than the TiO_2 layer. This effect, which has been refer to as the halogen effect, has been observed specifically in γ-TiAl intermetallics [12-15] and some Ni alloys [16, 17]. Different halogen and halides such as chlorine [10, 18, 19], fluorine [20, 21], bromide [9, 10], and iodide [9, 10], and treatment methods such ion implantation [22, 23] and plasma immersion ion induction [18] have been explored. A similar effect has been observed for treatments of Ti intermetallics with NaCl vapour [24, 25], dilute HF acid solutions [21, 26], $MnCl_2$ water solution [27], and gaseous fluorination [28, 29].

It has been reported, that the halogen effect does not work for Al concentrations of less than about 40 at% because of the insufficient concentration of Al necessary for activating the halogen effect [30]. However superior oxidation resistance of in Ti alloys with as little as 25 at% Al using different halide treatment methods has been reported [31] and there are some indications that a similar effect can be produced on titanium alloys during pack cementation [32].

Considering this, the main objective of this work focuses on the study of the halogen effect applied with methods other than ion implantation in the alloy Ti-6Al-4V produced by powder metallurgy route and subjected to high temperature oxidation and electrochemical corrosion in aeronautical environments.

At present there is a growing interest in the Ti alloy processed by powder metallurgy (PM), for its advantages in terms of material savings, obtaining the final shape parts, or the possibility of designing alloys with tailored compositions, which involves a considerable cost reduction. Recent advances in the production of Ti are mainly directed towards the production of low cost and high quality powders making possible the use of powder metallurgy for the manufacture of metal components for the aeronautic industry. In this context, this research aims to study the possible improvement of the oxidation and corrosion resistance of the titanium alloy Ti-6Al-4V obtained by powder metallurgy by application of halide surface treatments with ammonium chlorides. For comparative purposes, the same oxidation treatment was applied to cold rolled wrought alloy.

Materials and Methods

Metallic substrates

Ti-6Al-4V samples with nominal composition of 5.5 -6.76 wt % Al, 3.5-4.5 wt% V, 0.25 wt.% Fe (max.), 0.2 wt % O (max) were used. The samples were produced by conventional powder metallurgy. The powders were compacted in a double effect uniaxial press at 600 MPa, obtaining cylindrical disks of about 16 mm diameter and 3 mm thick, using zinc stearate as a wall-die lubricant. Sintering was carried out in a vacuum furnace at a pressure of about $2x10^{-5}$ mbar for 2 hours to 1200°C. Moreover, wrought Ti-6Al-4V substrates produced by rolling with dimensions of 10x15x1 mm were also used. All samples were ultrasonically cleaned in alcohol and dried prior to halide treatment.

Thermodynamic calculations

Thermodynamic studies of the phase equilibrium were performed using Thermocalc Software [33] to provide useful guidelines for optimizing the halide treatment. Calculations are based on the Gibbs free energy minimization code, in combination with Thermo-Calc Software SSUB4 Substances database version 4.

Halide Treatment

For carrying out the halide surface treatment the powder metallurgy samples and wrought samples were placed in a semi-sealed container containing a powder mixture, consisting of 3 wt% of the halide compound NH_4Cl, the remainder being inert filler (Al_2O_3). The powder mixture was homogenized prior to the treatment in a Turbula® multidirectional mixer for 1 hour. The semi-sealed container was heated in an inert argon atmosphere following the subsequent cycle: 1) a preliminary step of heating to 100°C where the samples were held for 30 minutes to remove moisture from NH_4Cl; 2) heating to the final temperatures of 200°C and 950°C, respectively, where the samples were maintained for 2 hours, and 3) a final cooling step to room temperature. The heating rate was 5ºC/min during all the steps and argon atmosphere was maintained throughout the cycle.

Oxidation Tests

Isothermal oxidation tests were conducted in a muffle furnace, under static air at 600ºC for a total of 300h. The samples subjected to the oxidation tests were powder metallurgy Ti6Al4V samples with halide surface treatment performed at 200ºC and 950ºC. For comparative purposes untreated wrought and powder

metallurgy Ti6Al4V samples were also oxidized. In addition, in order to establish the effect of the thermal treatment on the oxidation behaviour, samples treated at the same temperatures, without the presence of NH_4Cl were also subjected to the oxidation tests. Five samples for each of the conditions were used in order to obtain a representative measurement for each case. The samples were introduced into the furnace chamber, maintained at temperature for the specified time, cooled to room temperature inside the furnace, taken out, weighted, re-introduced into the furnace and re-heated to the test temperature. . In all the cases, samples were placed into the furnace in a specially designed holder ensuring all the surface area of the samples was exposed to air. The balance used for the weight measurements had an accuracy of 0.0001 gr.

Characterization techniques

X-Ray diffraction was performed using a Siemens D5000 diffractometer with monochromatic Cu Kα radiation. The cross-section of the samples was characterized by scanning electron microscopy (Philips XL 30) coupled with energy dispersive X-Ray spectroscopy (EDX). Prior to cutting the treated samples a Cu layer was applied by electrodeposition in order to protect the underlying coatings/oxides during metallographic preparation. Standard metallographic preparation was performed on samples prior to cross-section observations including grinding with SiC abrasive paper and polishing with 1 micron Al_2O_3 powder.

Electrochemical Corrosion

The corrosion behaviour of the samples was studied by electrochemical impedance spectroscopy (EIS). Tests were carried out by immersion of samples in dilute aerated Harrison aqueous solution at room temperature and with pH = 6.43. This solution is typically used to simulate in-service conditions for metallic samples in aeronautical environments and is composed of a 0.35 wt% $(NH_4)_2SO_4$ and 0.05 wt% NaCl. To perform the impedance measurements a conventional three-electrode configuration was used consisting of Pt counter electrode, Ag/AgCl (KCl, 3M) reference electrode (+210 mV vs Standard Hydrogen Electrode, SHE at 25ºC) and the Ti6Al4V wrought or powder metallurgy samples as working electrode.

The area exposed to the electrolyte was 1.5 cm^2. Impedance measurements were performed at room temperature in a Faraday cage, with a potentiostat PGSTAT302N in combination with a module FRA32M from Metrohm Autolab (EcoChemie). Open circuit measurements (OCP) were performed and the potential was held potenciostatically. Before performing the impedance measurements, it is verified that the potential remained stable for at least five minutes. In addition,

after the measurement it was confirmed that the potential was the same as the initial potential. During the running of the impedance tests the frequency range applied was from 10^5 Hz to 10^{-2} Hz. Impedance spectra were recorded at OCP, using logarithmic sweeps of five points per decade and 10 mV peak-to-peak sinusoidal voltage signals.

Results and Discussion

Thermodynamic calculations

Thermodynamic equilibrium calculations of the phases formed at different temperatures for the pack composition used were performed using Thermocalc software in order to determine the appropriate temperature for the halide treatment.

Figure 1a shows the phases formed in equilibrium considering a titanium substrate and a pack mixture containing 3 wt % NH_4Cl at atmospheric pressure, as a function of temperature. The inert Al_2O_3 filler was not taken into consideration in the calculation. Two regions can be observed: at temperatures below about 800ºC titanium chlorides and titanium hydride appears to be stable, whereas at above 800ºC a higher amount of gaseous species appear to be formed. The alloying elements of the titanium substrate material were not taking into consideration for this calculation. The equilibrium phases formed considering a titanium substrate and the alloying elements (Al and V) in a pack mixture containing 3 wt % NH_4Cl as a function of temperature are shown in Figure 1b. In this case it can be observed that there are three distinct regions: one at temperature below 500ºC where high amount of gas species and TiH_2 appear to be stale, one between 500-850ºC where $TiCl_2$ and TiAl phases appear to be stable, and the amount of gas species decreases and a region above 850ºC, where again an increase in the amount of gas phases is observed. In all cases the amount of stable compounds remains stable above 900ºC. Another consideration is the β transus temperature of PM-Ti-6Al-4V, in order to investigate the effect of substrate structure. The nominal β transus transformation for Ti-6Al-4V is 996ºC however for PM-Ti-6Al-4V the temperature of β transus is around 906ºC, most likely due to the in homogeneity of the starting powder [34]. Taking into consideration these results two different temperatures were chosen in order to perform halide treatment, corresponding to the regions observed in the thermodynamic calculations of stable phases: 200ºC and 950ºC.

Microstructure of samples after heat treatment

The cross sections of the samples treated at 200ºC and 950ºC in pack mixture containing 3wt% NH_4Cl are presented in Figure 2. The sample that was treated at 200ºC in the presence of NH_4Cl (Figure 2a) does not show any noticeable changes in the surface layer, only the protective outer Cu layer and the underlying substrate can be observed. X-ray diffraction confirms that the only phases present are alpha and beta titanium (Figure 3a). As it is common in all titanium alloys a very thin titanium oxide layer is most probably present at the surface, nevertheless, no other considerable characteristics can be observed. In the sample that was heat treated at 950ºC with NH_4Cl three different layers are visible. EDX analysis of the different regions in this sample is presented in table 1. The outer bright layer is the protective Cu layer applied for protection during metallographic preparation. The second layer contains some darker angular non-continuous regions (point 2a in Figure 2b) which correspond to aluminium oxide and a lighter region (region 2b in Figure 2b) which corresponds to titanium oxide. This layer is a result of the oxidation of the sample during the heat treatment. Even though the heat treatments where conducted in an argon atmosphere, possibly some oxygen still remains present. The formation of the aluminium oxide could possibly be attributed to the desired halogen effect, where the generation of aluminium chlorides changed the oxidation kinetics causing a preferential oxidation of the aluminium with respect to titanium. However, it is also possible that this oxide originates from the aluminium oxide that was present in the powder mixtures and considered to be inert. It is possible that during the heat treatment in the presence of the halide, aluminium oxide particles form the pack have become embedded within the titanium oxide layer. The inner layer (layer 3 in Figure 2b) consists mainly of titanium and oxygen and some nitrogen is also detected (point 3a in Figure 2b). It is possible that a TiN is formed, as the formation of a similar layer during pack cementation heat treatments of titanium alloys has previously been observed [32] and is thermodynamically favourable. The pores visible in this area are most probably due to reaction of titanium with NH_4Cl and the formation titanium chlorides [32]. In this inner layer there are darker areas within the pores that appears to contain a small amount of Cl (point 3b in Figure 2b) that possibly originates for the NH_4Cl that was present in the powder mixture. X-ray diffraction confirms the presence of Al_2O_3, TiO_2 (Figure 3b).

Oxidation behaviour of samples treated at 200ºC

The mass gain with respect to oxidation time for the samples heat treated at 200ºC with 3 wt% NH_4Cl is presented in Figure 4. In the same graph the oxidation curves for the samples heat treated at 200ºC without NH_4Cl and the untreated Ti6Al4V

powder metallurgy sample are also shown. Error bars represent the standard deviation since measurements were performed for five samples in each case. The sample that has been treated without the presence of NH_4Cl shows the highest weight gain, indicating the lowest oxidation resistance, followed by the untreated samples which have a mass gain of approximately 1.5 mg/cm^2. The samples with halide treatment show the lowest weight gain, approximately 1 mg/cm^2, indicating an increase in oxidation resistance. It is worth noting that it appears that the heat treatment at 200ºC itself appears to have been detrimental for the oxidation resistance, compared to the untreated sample, whereas when the same heat treatment is performed in the presence of NH_4Cl the oxidation resistance is noticeably better.

The cross sections of the samples that were treated at 200ºC with and without NH_4Cl after 300h at 600ºC are shown in Figure 5. The EDX analysis of the oxide layers and the XRD analysis are presented in tables 2 and 3 and Figure 6 respectively.

Three layers are observed in the halide treated sample: the layer 1 in figure 5a corresponds to the protective Cu coating that was applied in order to protect the sample during metallographic preparation, whereas layer 3 in figure 5a corresponds to the substrate. The oxide layer (layer 2 in figure 5a) is predominantly titanium oxide, about 10 microns thick and consists of two sublayers: a slightly darker upper sublayer (sublayer 2a) where there is a higher concentration of aluminium and sublayer 2b which consist of titanium oxide and no aluminium is present (table 2). In the sample that has been heat treated without NH_4Cl, layer 1 in figure 5b corresponds to the Cu protective layer, layer 3 in figure 5b is the substrate and the layer 2 in figure 5b is the oxide layer, which is about 5 μm thick and consists of titanium oxide (table 3). Comparing the composition of the cross sections of the samples treated at 200°C in the presence of NH_4Cl and in the absence of NH_4Cl, it can be seen that the samples treated with NH_4Cl there is an outer layer richer in aluminium that is not present for the samples treated samples without NH_4Cl. The X-ray diffraction spectra of samples heat treated at 200ºC both in the presence of NH_4Cl and without NH_4Cl after oxidation for 300 hour in air at 600ºC are very similar and confirm the presence of TiO_2, Ti and some Al_2O_3 in both cases (figure 6).

Oxidation behaviour of samples treated at 950ºC

The oxidation curves of the powder metallurgy samples treated at 950°C (both in the presence of NH_4Cl and without NH_4Cl), along with oxidation curve of the untreated Ti6Al4V powder metallurgy samples, taken as a reference material, are

represented in Figure 7. Error bars represent the standard deviation since measurements were performed for five samples in each case.

The samples heat treated at 950ºC in absence of NH_4Cl shows significant weight gain and a noticeable decrease in oxidation resistance. On the other hand, it can be seen in the curve of samples treated with NH_4Cl, shows initially some mass loss, which might be due the volitisation of some components upon exposure to air at high temperature. No spalling of oxide was observed, or other visible deterioration, but it might be possible that local partial detachment of the coating occurred.

The approximate values of mass gain of 300 hours of oxidation are about 1.2 mg/cm^2 for the case of untreated sample, about 5.2 mg/cm^2 for the case of sample treated in the absence of NH_4Cl, and about 0.7 mg/cm^2 in the case of samples treated with NH_4Cl. The differences are significant, and an evident decrease in oxidation resistance is observed when a heat treatment in absence of NH_4Cl is performed, whereas when the sample is heat treated in the presence of NH_4Cl, not only are the negative effects averted but a possible beneficial effect in the oxidation resistance with respect to the untreated sample might be observed.

Figure 8a shows the cross sections of Ti6Al4V powder metallurgy sample treated for 2h a 950°C with NH_4Cl, after 300h at 600ºC in air and the EDX analysis is presented in table 4. The cross section appears very similar to the cross section of the sample heat treated at 950ºC with NH_4Cl prior to the oxidation heat treatment (figure 2b). No appreciable changes appear in the layers present. There is a darker region (point 2 in Figure 8a) corresponding to aluminium oxide, a dark grey layer (point 3 in Figure 8a) corresponding to titanium oxide, and an inner layer that contains Ti and N. This is in agreement with the observed oxidation curves where very little mass gain was detected. The only appreciable difference might be the slightly more continuous nature of the alumina blocks. It appears that the halide treatment resulted in a layered structure that remains relative stable during oxidation for 300h in air and prevents further oxidation of the substrate. X-ray diffraction confirmed the presence of aluminium oxide (Al_2O_3) mainly and traces of titanium oxide (rutile) (it possible that the small remaining unidentified peaks correspond to $Al_8O_3N_6$) (Figure 9a). In contrast the sample that was heat treated at 950 without NH_4Cl shows mainly titanium oxide (Figure 9b).

The cross section of the sample was that was treated at 950ºC without NH_4Cl after oxidation is shown in Figure 8b and the EDX analysis is presented in table 5. It can be seen that a thick oxide layer is formed about 15 µm thick that consists of titanium oxide. It is possible that the outer region (point 2 in Figure 8b) contains a

higher amount of aluminium (table 5). The mass gain in this sample was considerably greater than in the untreated sample, indicating a lower oxidation resistance.

Comparison of oxidation behaviour of powder metallurgy and wrought samples

Figure 10 shows the mass gain with respect to oxidation time for the Ti6Al4V powder metallurgy and wrought untreated sample. In general wrought samples have better oxidation behaviour, and after 300 hours powder metallurgy samples have a mass gain of about 1.2 mg/cm^2, while in the case of the wrought samples, they reach a mass gain of about 1 mg/cm^2; this difference although not too large is noticeable. The cross section of the samples, shown in figure 11, is very similar in both cases, showing and oxide layer about 6-10 μm in thickness, consisting mainly of titanium oxide. EDX analysis of both samples is shown in Tables 6 and 7, respectively. It is worth noting that within this layer an outer sublayer on about 3 μm can be observed that contains a slightly higher amount of Al (points 2a in Figure 11a and 11b). X-ray diffraction confirms the presence of titanium oxide in both samples (Figure 12). In both cases the oxide layer is smaller than the layer observed in the sample treated at 950ºC without NH_4Cl that shows considerable worse oxidation behaviour. However, the layer is very similar to the layers observed in the samples treated at 200ºC (both with and without NH_4Cl). The most noticeable difference lies on the slightly higher concentration of Al in the outer layer of the sample treated with NH_4Cl at 200ºC, which shows the best oxidation behaviour. The mechanism proposed for this difference in oxidation behaviour in the halide treated Ti-6Al-4V alloy at 200ºC may be similar to the halogen effect mechanism proposed for higher Al containing alloys[9, 12, 13] i.e the formation of gaseous aluminium halides which oxidize and activate a mechanism of selective oxidation of aluminium. This leads to a change in the oxidation kinetics from fast oxidation kinetics that cause the formation of a mixed oxide layer of TiO_2 and Al_2O_3 to slow oxidation kinetics in which only the aluminium is oxidized.

Electrochemical Corrosion

The electrochemical corrosion was analysed by using electrochemical impedance spectroscopy measurements. These tests were carried out at Open Circuit Potential (OCP) in potentiostatic mode. Before performing the impedance measurements, it is verified that steady state was reached the potential remained stable for at least five minutes. In addition, after the measurement it was confirmed that the potential was the same as the initial potential. The most representative potential variations

were OCP_{300s} = OCP_{0s}± 2 mV. Table 8 shows the OCP values determined for each samples before starting the EIS measurement.

Figure 13 shows the impedance diagrams of the specimens produced by powder metallurgy obtained after 5 hours of immersion in Harrison' dilute solution. The representation of the impedance data as Nyquist diagram shows that the specimen treated at 200°C in the presence of NH_4Cl has an arch more open than the other samples (Figure 13 a and b). In the double logarithmic representation of the module of impedance versus frequency (Bode plot), the same effect is markedly reflected in the high impedance values recorded at low frequencies compared to the impedance values observed for the rest of the samples (Figure 13 c and d). The thermochemical treatment applied to the sample instigates a protective action against electrochemical corrosion which is reflected in the high impedance values observed for these samples in the low and middle frequency regions.

After 4 days immersion in Harrison' dilute solution similar effects as those registered for short exposure times are observed (Figure 14). The samples treated for 2h at 200ºC with NH_4Cl present an open arc in the Nyquist diagram (Figures 14a and b) and an impedance module highest than for the rest of the samples tested is observed in the low frequencies region of the Bode plots (Figure 14 c). The phase angle of this sample shows also the highest values into the $2{\cdot}10^{-1}$-10^{4} frequency region (Figure 14d).

In Figure 15 the impedance plots Ti6Al4V wrought and powder metallurgy samples heat-treated at 200ºC with NH_4Cl are compared after 4 days of the immersion test in Harrison dilute solution. In both cases Nyquist diagrams show two arcs (Figures 15a and 15b). The representation of the impedance module in the Bode diagrams shows two dwellings (Figure 15c). One of them is observed at high frequencies and the other one at the lowest frequencies. At middle frequencies a straight line whose slope approaches a value close to -1 is observed (Figure 15c). At frequencies set around 10 Hz the presence of an inflection point is observed, associated with two phenomena that are masked, and as a consequence variations in phase angle versus frequency in semi-logarithmic representation describe a deformed bell (Figure 15d). This behavior is typically ascribed to the impedance response of phenomena associated with distribution elements [35]. On this case, the Nyquist diagram layout, more clearly reveals the existence of two phenomena with differentiated relaxation times. The time constant associated with the phenomenon of high-frequencies is due to the impedance response of a resistor and a capacitor (RC) which are connected in parallel. The value of this time constant is determined

by the intrinsic electrical properties of the oxide layer (i.e. its dielectric constant and electrical conductivity). On the other hand the time constant associated with the low-frequency phenomenon is due to another couple of electrical elements (RC) which is also connected in parallel. The value of this new constant time is actually governed by kinetics of the electrochemical corrosion processes of the metal substrate at the base of the pores and cracks of the oxide layer, immersed in the solution of Harrison.

In Figure 15 it can also be clearly observed that in all tested frequency regions the impedance value of wrought sample is one order of magnitude higher than the values obtained for the PM sample. This behaviour indicates that the alloy produced by rolling has better performance against corrosion than the samples manufactured by conventional powder metallurgy, probably due to a disadvantageous effect provoked by the presence of pores in the PM manufacturing process. In view of the good results achieved with this sample a deeper analysis of the impedance diagrams was performed. The best fitting of the impedance diagrams was obtained using the equivalent circuit shown in Figure 16. In this circuit Rs represents the resistance of the electrolytic Harrison solution, Ccoat is a capacitor associated with the dielectric properties of the oxide generated by the thermochemical treatment. Note that Ccoat has been implemented with a constant phase element (CPE), for taking into account the non-ideal behaviour of this capacitor. The disappearance from the ideal behaviour is probably due to surface roughness or heterogeneities present in the oxide layer produced during the heat treatment of the samples tested. Rcoat represents the resistance of the electrolyte inside the pores and cracks of the coating. Cdc describes the non-ideal behaviour of the electrochemical double layer formed in the metal/electrolyte interface. In this equivalent circuit Cdc is also implemented with a CPE. Finally, the resistance Rcorr is associated with charge transfer resistance into the interface metal/electrolyte, which is inversely related to the corrosion rate of the metal substrate [36, 37].

Table 9 shows that the phase angle values at the 10 MHz frequency are low for all samples tested. Therefore, for this frequency, the values of the modulus of the impedance vector are predominantly influenced by the resistive component of this vector. Thus, to a first approximation, one can use the parameter $|Z|_{10mHz}$ for classification of the corrosion behaviour of the samples tested, depending on the surface treatment applied.

Table 9 also shows that the values of the parameter $|Z|_{10mHz}$ for the Ti6Al4V PM untreated sample increased significantly during the immersion test in Harrison's dilute solution from 676 $\Omega \cdot cm^2$ at 5 hours of immersion to 1543 $\Omega \cdot cm^2$ after 4 days of immersion. This effect is probably due to the spontaneous passivation of the oxide layer of these samples when in contact with dilute Harrison's solution, producing a growth of the oxide layer. The increased thickness of the layer leads to an improvement of the barrier property against corrosion, which is reflected in the increased values of the $|Z|_{10mHz}$ parameter. A similar effect is produced for the sample treated at 200°C without NH_4Cl (Table 9). By contrast the treatment of 950°C produces a porous and cracked oxide layer in the samples treated without NH_4Cl which cuases a decrease in the values of the parameter $|Z|_{10mHz}$ with increasing immersion time in Harrison's dilute solution from 5 hours to 4 days.

The best results from the point of view of resistance to corrosion (i.e., those associated with higher values of $|Z|_{10mHz}$) correspond to the sample subjected to a heat treatment at 200°C in presence of NH_4Cl, as a result of the halogen effect.

By contrast, the samples treated at 950°C in presence of NH_4Cl do not exhibit neither the barrier effect (i.e. halogen effect) nor the effect of spontaneous passivation observed in the untreated and/or the samples treated at 200°C without NH_4Cl. This unfavourable behaviour may be due to the presence of cracks and pores caused by the oxide layer generated during the heat treatment at 950°C in presence of NH_4Cl, as observed in Figure 8a.

Table 10 summarizes the numerical values obtained for each of the electrical elements of the equivalent circuit proposed for the wrought and the PM Ti6Al4V samples heat-treated at 200ºC with NH_4Cl after 4 days of immersion in dilute Harrison's solution. These calculations are based on the analysis of the impedance data in the complex plane by using numerical iteration methods of complex nonlinear least squares fitting (CNLS) and available routines of the Zview commercial software. It can be seen that the relative errors in the calculations are quite low. Likewise, it is observed that the chi-square value obtained for the wrought sample is also very low ($2.46x10^{-4}$) which indicates that the quality of the fits obtained is very satisfactory. On the other hand the high frequency impedance arc obtained for the PM sample is very indefinite. Thus only the impedance response for the low and middle frequencies can be analyzed. Table 10 shows that in the case of the wrought samples the obtained fits are also very satisfactory. It can be observed that the corrosion resistance (Rcorr) of the wrought sample is 21.2 times higher than the measured values for the PM Ti6Al4V sample.

Conclusions

Appropriate temperatures for performing a simple halide treatment on Ti-6Al-4V heat treatment using NH_4Cl were identified using thermodynamic calculations. When the halide heat treatment was performed at 950ºC the coating exhibited two distinct layers. The top layer consisted of TiO_2 with some Al_2O_3 blocks and the inner layer had some porosity possibly attributed to attack of the substrate by NH_4Cl. Heat treatment at 200ºC did not modify the substrate noticeably.

Oxidation tests in air at 600ºC for 300h showed that treatment with NH_4Cl at 200ºC increases oxidation resistance. Samples treated with NH_4Cl at 200ºC showed an outer oxide layer enriched with aluminium.

Measurements made with the technique of electrochemical impedance showed that PM Ti6Al4V samples treated at 200°C in the presence of NH_4Cl have the best performance in immersion tests in dilute Harrison solution. The values of the parameter $|Z|_{10mHz}$, directly related to the corrosion resistance, for these samples are higher, both at short exposure times (5 hours) in the electrolyte medium and at long times, a marked effect compared to the other PM samples. Treatment at 950° C does not produce an improvement in the susceptibility to electrochemical corrosion of the samples.

Both oxidation and electrochemical tests showed that wrought Ti6Al4V samples treated at 200°C with NH_4Cl showed better corrosion and oxidation resistance than powder metallurgy samples with the same heat treatment. It can be concluded that halide treatment at 200ºC with NH_4Cl increases resistance against oxidation at high temperatures and corrosion in conditions simulating aircraft environments (Harrison dilute solution) showing promising results.

Acknowledgements

The authors wish to thank the Ministry of Education and Science for funding through R & D project MAT2012-38650-C02-01, and the Community of Madrid for its funding through ESTRUMAT program (S-2009/MAT-1585).

References

[1] E. Galvanetto, F.P. Galliano, A. Fossati, F. Borgioli, Corrosion resistance properties of plasma nitrided Ti-6Al-4V alloy in hydrochloric acid solutions, Corrosion Sci., 44 (2002) 1593-1606.

[2] Z.G. Zhang, Y.P. Peng, Y.L. Mao, C.J. Pang, L.Y. Lu, Effect of hot-dip aluminizing on the oxidation resistance of Ti-6Al-4V alloy at high temperatures, Corrosion Sci., 55 (2012) 187-193.

[3] X.L. Zhang, Z.H. Jiang, Z.P. Yao, Z.D. Wu, Electrochemical study of growth behaviour of plasma electrolytic oxidation coating on Ti6AI4V: Effects of the additive, Corrosion Sci., 52 (2010) 3465-3473.

[4] L. Wenbo, Z. Shenglong, W. Cheng, C. Minghui, S. Mingli, W. Fuhui, SiO 2-Al 2O 3-glass composite coating on Ti-6Al-4V alloy: Oxidation and interfacial reaction behavior, Corrosion Sci., 74 (2013) 367-378.

[5] M.R. Amaya-Vazquez, J.M. Sanchez-Amaya, Z. Boukha, F.J. Botana, Microstructure, microhardness and corrosion resistance of remelted TiG2 and Ti6Al4V by a high power diode laser, Corrosion Sci., 56 (2012) 36-48.

[6] V. Jokanovic, M. Vilotijevic, B. Jokanovic, M. Jenko, I. Anzel, D. Stamenkovic, V. Lazic, R. Rudolf, Investigations of corrosion on the surface of titanium substrate caused by combined alkaline and heat treatment, Corrosion Sci., 82 (2014) 180-190.

[7] M. Chen, W. Li, M. Shen, S. Zhu, F. Wang, Glass-ceramic coatings on titanium alloys for high temperature oxidation protection: Oxidation kinetics and microstructure, Corrosion Sci., 74 (2013) 178-186.

[8] A. Donchev, E. Richter, M. Schuetze, R. Yankov, Improvement of the oxidation behaviour of TiAl-alloys by treatment with halogens, Intermetallics, 14 (2006) 1168-1174.

[9] M. Schutze, G. Schumacher, F. Dettenwanger, U. Hornauer, E. Richter, E. Wieser, W. Moller, The halogen effect in the oxidation of intermetallic titanium aluminides, Corrosion Sci., 44 (2002) 303-318.

[10] M. Kumagai, K. Shibue, M.S. Kim, M. Yonemitsu, Influence of chlorine on the oxidation behavior of TiAl-Mn intermetallic compound, Intermetallics, 4 (1996) 557-566.

[11] A. Donchev, M. Schuetze, Improving the oxidation resistance of gamma-titanium aluminides by halogen treatment, Materials and Corrosion-Werkstoffe Und Korrosion, 59 (2008) 489-493.

[12] A. Donchev, B. Gleeson, M. Schutze, Thermodynamic considerations of the beneficial effect of halogens on the oxidation resistance of TiAl-based alloys, Intermetallics, 11 (2003) 387-398.

[13] M. Schutze, M. Hald, Improvement of the oxidation resistance of TiAl alloys by using the chlorine effect, Mater. Sci. Eng. A-Struct. Mater. Prop. Microstruct. Process., 240 (1997) 847-858.

[14] G. Schumacher, F. Dettenwanger, M. Schutze, U. Hornauer, E. Richter, E. Wieser, W. Moller, Microalloying effects in the oxidation of TIAl materials, Intermetallics, 7 (1999) 1113-1120.

[15] S. Taniguchi, Oxidation of intermetallics - Japanese activity, Materials and Corrosion-Werkstoffe Und Korrosion, 48 (1997) 1-9.

[16] H.E. Zschau, P.J. Masset, M. Schuetze, Oxidation protection of Ni-base superalloys by halogen treatment, Materials and Corrosion-Werkstoffe Und Korrosion, 62 (2011) 687-694.

[17] H.-E. Zschau, D. Renusch, P.J. Masset, M. Schuetze, The halogen effect for Ni-base alloys - A new method for increasing the oxidation protection at high temperatures, Nuclear Instruments & Methods in Physics Research Section B-Beam Interactions with Materials and Atoms, 267 (2009) 1662-1665.

[18] U. Hornauer, E. Richter, E. Wieser, W. Moller, A. Donchev, M. Schutze, Plasma immersion ion implantation of TiAl using chlorine containing plasma, Surface & Coatings Technology, 174 (2003) 1182-1186.

[19] M. Kumagai, K. Shibue, M.S. Kim, INFLUENCE OF MINOR ELEMENTS ON OXIDATION BEHAVIOR OF TIAL INTERMETALLIC COMPOUND, Journal of the Japan Institute of Metals, 57 (1993) 721-725.

[20] S. Neve, K. Stiebing, L.P.H. Schmidt, H.-E. Zschau, P.J. Masset, M. Schuetze, Non-destructive fluorine depth profiling as quality assurance for the oxidation protection of TiAl turbine blades, in: T. Chandra, N. Wanderka, W. Reimers, M. Ionescu (Eds.) Thermec 2009, Pts 1-4, 2010, pp. 1384-1389.

[21] H.-E. Zschau, M. Schuetze, H. Baumann, K. Bethge, Surface modification of titanium aluminides with fluorine to improve their application for high temperature service conditions, Nuclear Instruments & Methods in Physics Research Section B-Beam Interactions with Materials and Atoms, 257 (2007) 383-387.

[22] U. Hornauer, E. Richter, E. Wieser, W. Moller, G. Schumacher, C. Lang, M. Schutze, Improvement of the high temperature oxidation resistance of Ti50Al via ion-implantation, Nuclear Instruments & Methods in Physics Research Section B-Beam Interactions with Materials and Atoms, 148 (1999) 858-862.

[23] S. Neve, P.J. Masset, R.A. Yankov, A. Kolitsch, H.-E. Zschau, M. Schuetze, High temperature oxidation resistance of fluorine-treated TiAl alloys: Chemical vs. ion beam fluorination techniques, Nuclear Instruments & Methods in Physics Research Section B-Beam Interactions with Materials and Atoms, 268 (2010) 3381-3385.

[24] M. Hara, Y. Kitagawa, Effect of trace amounts of NaCl vapor on high-temperature oxidation of TiAl, Oxid. Met., 52 (1999) 77-94.

[25] Y. Xiong, S. Zhu, F. Wang, Synergistic corrosion behavior of coated Ti60 alloys with NaCl deposit in moist air at elevated temperature, Corrosion Sci., 50 (2008) 15-22.

[26] H.E. Zschau, V. Gauthier, G. Schumacher, F. Dettenwanger, M. Schutze, H. Baumann, K. Bethge, M. Graham, Investigation of the fluorine microalloying effect in the oxidation of TiAl at 900 degrees C in air, Oxid. Met., 59 (2003) 183-200.

[27] L. Xin, G. Shao, F. Wang, P. Tsakiropoulos, T. Li, Improving high-temperature oxidation resistance of TiAl-based alloys by MnCl2 surface treatment, Intermetallics, 11 (2003) 651-660.

[28] K. Shibue, M. Kim, M. Kumagai, Titanium aluminide having improved oxidn. resistance|prepd. from powder mixt. to wave intergranular and adherent surface oxide films, in, Sumitomo Light Metal Ind Co.

[29] A. Donchev, E. Richter, M. Schuetze, R. Yankov, Improving the oxidation resistance of TiAl-alloys with fluorine, Journal of Alloys and Compounds, 452 (2008) 7-10.

[30] R.A. Yankov, A. Kolitsch, J. von Borany, A. Muecklich, F. Munnik, A. Donchev, M. Schuetze, Surface protection of titanium and titanium-aluminum alloys against environmental degradation at elevated temperatures, Surface & Coatings Technology, 206 (2012) 3595-3600.

[31] M. Kumagai, K. Shibue, M. Kim, T. Furuyama, Titanium@-aluminium@ intermetallic cpd. - having superior resistance to wear and to oxidn. and contg. at least one halogen element and dense alumina surface film, in, Sumitomo Light Metal Ind Co (Sumk), pp. 580081-B580081:.

[32] S.A. Tsipas, M.R. Vazquez-Alcazar, E.M. Ruiz Navas, E. Gordo, Boride coatings obtained by pack cementation deposited on powder metallurgy and wrought Ti and Ti-6Al-4V, Surface & Coatings Technology, 205 (2010) 2340-2347.

[33] J.O. Andersson, T. Helander, L.H. Hoglund, P.F. Shi, B. Sundman, THERMO-CALC & DICTRA, computational tools for materials science, Calphad-Computer Coupling of Phase Diagrams and Thermochemistry, 26 (2002) 273-312.

[34] L. Bolzoni, P.G. Esteban, E.M. Ruiz-Navas, E. Gordo, Mechanical behaviour of pressed and sintered titanium alloys obtained from prealloyed and blended elemental powders, Journal of the Mechanical Behavior of Biomedical Materials, 14 (2012) 29-38.

[35] F. Mansfeld, Y. Wang, H. Shih, The Ce-Mo process for the development of a stainless aluminum, Electrochimica Acta, 37 (1992) 2277-2282.

[36] A. Jimenez-Morales, P. Aranda, J.C. Galvan, Nanocomposite materials based on organopolysiloxane/macrocyle systems for electrochemical sensors, Journal of Materials Processing Technology, 143 (2003) 5-10.

[37] A. Jimenez-Morales, J.C. Galvan, P. Aranda, A new silver-ion selective sensor based on a polythiacrown-ether entrapped by sol-gel, Electrochimica Acta, 47 (2002) 2281-2287.

Figure Captions

Figure 1. Mass fraction of solid phases as a function of temperature for pack mixture containing 3wt % NH_4Cl in the presence of a)Ti and b) Ti 6Al-4V

Figure 2. Backscattered electron image of cross section of Ti6Al4V powder metallurgy sample after thermochemical treatment for 2h with NH_4Cl at temperatures of a) 200°C and b) 950°C

Figure 3. X-ray diffraction patterns of Ti6Al4V powder metallurgy after thermochemical treatment for 2h with NH_4Cl at temperatures of a) 200°C and b) 950°C

Figure 4. Mass gain with respect to the exposure time in oxidation tests at 600 ºC of powder metallurgy samples treated with and without NH_4Cl at 200ºC compared to untreated Ti6Al4V PM samples

Figure 5. Backscattered electron image of cross section of Ti6Al4V powder metallurgy sample treated for 2h at temperature of 200°C a) with NH_4Cl, b) without NH_4Cl, after oxidation for 300h at 600ºC in air

Figure 6. X-ray diffraction patterns of Ti6Al4V powder metallurgy samples treated for 2h at temperature of 200ºC a) with NH_4Cl b) without NH_4Cl, after oxidation for 300 h at 600ºC in air.

Figure 7. Mass gain with respect to the exposure time in oxidation tests at 600ºC of powder metallurgy samples treated with and without NH_4Cl at 200ºC compared to untreated Ti6Al4V PM samples

Figure 8. Backscattered electron image of cross section of Ti6Al4V powder metallurgy sample treated for 2h at temperature of 950°C a)with NH_4Cl and b) without NH_4Cl ,after oxidation for 300h at 600ºC in air.

Figure 9. X-ray diffraction patterns of Ti6Al4V powder metallurgy samples treated for 2h at temperature of 950ºC a) with NH_4Cl b) without NH_4Cl, after oxidation for 300 h at 600ºC in air.

Figure 10. Mass gain with respect to the exposure time in oxidation tests at 600ºC of powder metallurgy Ti6Al4V untreated samples compared to wrought untreated Ti6Al4V samples

Figure 11a. Backscattered electron image of cross section of Ti6Al4V a) powder metallurgy and b) wrought untreated sample after 300h at 600ºC

Figure 12. X-ray diffraction patterns of a) powder metallurgy and b) wrought Ti6Al4V samples, after 300 h at 600ºC in air.

Figure 13. Nyquist and Bode plots for untreated and treated PM Ti6Al4V samples after 5 hours of immersion in Harrison dilute solution: a) Nyquist plot; b)detail of Nyquist plot; c) Bode plot of |Z| versus frequency; d) Bode plot of θ versus frequency. Frequency range applied: 10^{5} Hz to 10^{-2} Hz.

Figure 14. Nyquist and Bode diagrams of untreated and treated PM Ti6Al4V samples after 4 days of immersion in Harrison dilute solution: a) Nyquist plot; b)detail of Nyquist plot; c) Bode plot of |Z| versus frequency; d) Bode plot of θ versus frequency. Frequency range applied: 10^{5} Hz to 10^{-2} Hz.

Fig. 15. Nyquist and Bode diagrams obtained for heat-treated wrought and PM Ti6Al4V samples at 200ºC with NH_4Cl, after 4 days of immersion in Harrison dilute solution: a) Nyquist plot; b)detail of Nyquist plot; c) Bode plot of |Z| versus frequency; d) Bode plot of θ versus frequency. Frequency range applied: 10^{5} Hz to 10^{-2} Hz. OCPs: +34 mV for PM Ti6Al4V and +27 mV for Wrought Ti6Al4V (vs Ag/AgCl Ref. electrode), respectively.

Fig.16. Equivalent circuit proposed for adjustment of impedance behavior

Tables

Table 1. Analysis of composition (EDX) and characteristic features Ti6Al4V-PM treated at 950ºC with NH_4Cl, shown in Figure 2b.

Layer		Element (at%)						Characteristics of layer
		O	Al	Ti	Cl	N	V	
1								Cu protective layer
2	2a	51	49	-		-	-	Aluminium oxide discontinuous layer
	2b	58	1	41		-	-	Titanium oxide layer with some small porosity
	2c	55	2	34	2	-	7	Thin interface layer
3	3a	21	5	59	-	13	3	Titanium oxide and Titanium nitride
	3b	40	7	34	6	3	10	Darker areas within pores
4		-	12	84		-	4	Substrate

Table 2. Analysis of composition (EDX) and characteristic features Ti6Al4V-PM treated at 200ºC with NH_4Cl after 300h at 600ºC, shown in Figure 5a.

Layer		Element (at%)				Characteristics of layer
		O	Al	Ti	V	
1						Cu protective layer
2	2a	65	13	22	-	Denser layer, 5 - 10 μm thickness, titanium oxide, some Al present
	2b	65	1	35	-	Small porosity, 5 - 10 μm thickness, Titanium oxide
3						Substrate

Table 3. Analysis of composition (EDX) and characteristic features Ti6Al4V-PM treated at 200ºC without NH_4Cl after 300h at 600ºC, shown in Figure 5b.

Layer	Element (at%)				Characteristics of layer
	O	Al	Ti	V	
1					Cu protective layer
2	60	1	38	1	Point in the upper part of the layer: Small porosity, 5 - 10 μm thickness, Titanium oxide
	56	21	21	2	Some isolated small darker regions appear on the outer surface which are richer in Aluminium
3					Substrate

Table 4. Analysis of composition (EDX) and characteristic features Ti6Al4V-PM treated at 950ºC with NH_4Cl after 300h at 600ºC, shown in Figure 8a.

Layer	Element (%at)				Characteristics of layer
	O	Al	Ti	N	
1	-	-	-	-	Cu protective layer
2	48	52	-	-	Aluminum oxide discontinuous layer
3	56	3	41	-	Titanium oxide layer with some small porosity
4	59	-	41	-	Microporosity, thickness 5µm
5	21	5	57	17	Titanium oxide and Titanium nitride
6					Substrate

Table 5. Analysis of composition (EDX) and characteristic features Ti6Al4V-PM treated at 950ºC without NH4Cl after 300h at 600ºC, shown in Figure 8b.

Layer	Element (%at)				Characteristics
	O	Al	Ti	V	
1	-	-	-	-	Cu protective layer
2	57.39	20.20	22.01	0.40	Darker point in outer oxide layer with higher Al content
3	53.99	4.21	40.91	0.89	Titanium oxide layer about 15µm thick
4	-	11	84	5	Substrate

Table 6. Analysis of composition (EDX) and characteristic features Ti6Al4V-PM untreated, shown in figure 11a.

Layer		Element (%at)				Characteristics
		O	Al	Ti	V	
1		-	-	-	-	Cu protective layer
2	2a	59.92	7.79	31.83	0.46	Porous layer, 3-5 µm thickness, titanium oxide, some Al present
	2b	61.30	0.54	37.93	0.23	Titanium oxide 3µm thickness
3		-	-	-	-	Substrate

Table 7. Analysis of composition (EDX) and characteristic features Ti6Al4V-wrought untreated, shown in Figure 11b.

Layer		Element (%at)				Characteristics
		O	Al	Ti	V	
1		-	-	-	-	Cu protective layer
2	2a	60.61	8.84	30.20	0.35	Porous layer, 3-5 µm thickness, titanium oxide, some Al present
	2b	61.12	1.64	36.85	0.39	Titanium oxide 3µm thickness
3		-	-	-	-	Substrate

Table 8. Open Circuit Potential (OCP) values vs Ag/AgCl reference electrode for the different samples used for electrochemical impedance measurement for 5 hours and 4 days immersion time.

Thermal treatments	Immersion time in Harrison' dilute solution	
	5 hours	4 days
	OCP / mV	OCP / mV
Untreated sample	+ 102	+ 50
200ºC without NH_4Cl	+ 34	+ 57
200ºC in presence of NH_4Cl	+ 32	+ 51
950ºC without NH_4Cl	+ 57	+ 141
950ºC in presence of NH_4Cl	+ 102	+ 50

Table 9. Variations of the impedance module |Z| and phase angle θ at a constant frequency of 10 mHz for Ti6Al4V PM alloy as a function of the applied treatments for 5 hours and 4 days immersion time.

Thermal treatments	Immersion time in Harrison' dilute solution			
	5 hours		4 days	
	$\lvert Z\rvert$ / $\Omega\cdot cm^2$	θ / deg.	$\lvert Z\rvert$ / $\Omega\cdot cm^2$	θ / deg
Untreated sample	676	15	1543	15
200ºC without NH_4Cl	2172	12	3687	42
200ºC in presence of NH_4Cl	10900	8	7137	5
950ºC without NH_4Cl	3223	25	1140	15
950ºC in presence of NH_4Cl	2601	25	2105	21

Table 10. Values for the electrical elements of the equivalent circuit proposed in Figure 16, obtained for heat-treated wrought and PM Ti6Al4V samples at 200ºC with NH_4Cl, after 4 days of immersion in Harrison dilute solution.

	Wrought Ti6Al4V sample		PM Ti6Al4V sample	
Element	Value	% Error	Value	% Error
Rs ($\Omega\cdot cm^2$)	36.42	16.18	-	N/A
Ccoat-P	0.38	1.55	-	N/A
Ccoat-T ($\Omega^{-1}\cdot s^{-n1}\cdot cm^{-2}$)	$3.09\cdot10^{-5}$	6.68	-	N/A
Rcoat ($\Omega\cdot cm^2$)	5772	16.18	57.81	11.52
Cdl-P	0.72	0.76	0.71	0.76
Cdl-T ($\Omega^{-1}\cdot s^{-n2}\cdot cm^{-2}$)	$8{,}67\cdot10^{-6}$	0.91	$4.04\cdot10^{-5}$	2.11
Rcorr ($\Omega\cdot cm^2$)	$1.47\cdot10^{5}$	1.13	$6.94\cdot10^{3}$	0.94
Chi-square	$2.46\cdot10^{-4}$		$2.20\cdot10^{-3}$	

n1 is the exponent of the CPE associated to the coating capacitance (Ccoat-P)

n2 is the exponent of the CPE associated to the double layer capacitance (Cdl-P)

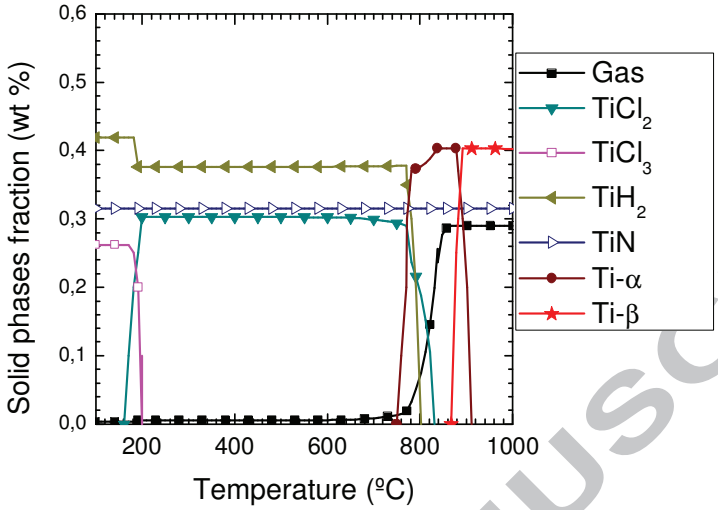

a)

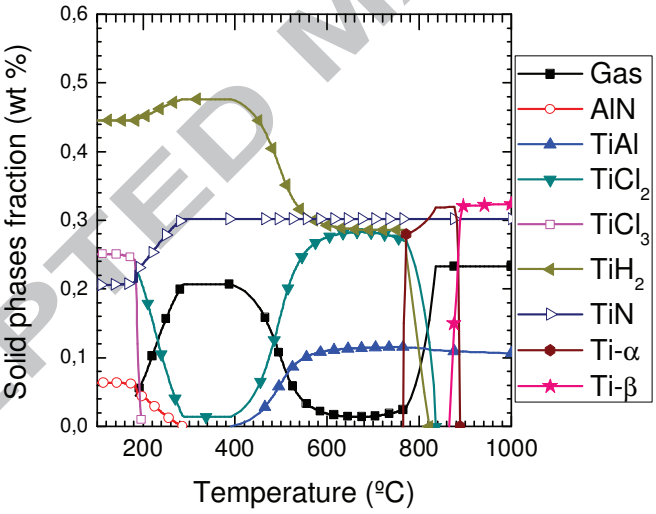

b)

Figure 1 Mass fraction of solid phases as a function of temperature for pack mixture containing 3wt % NH_4Cl in the presence of a)Ti and b) Ti 6Al-4V

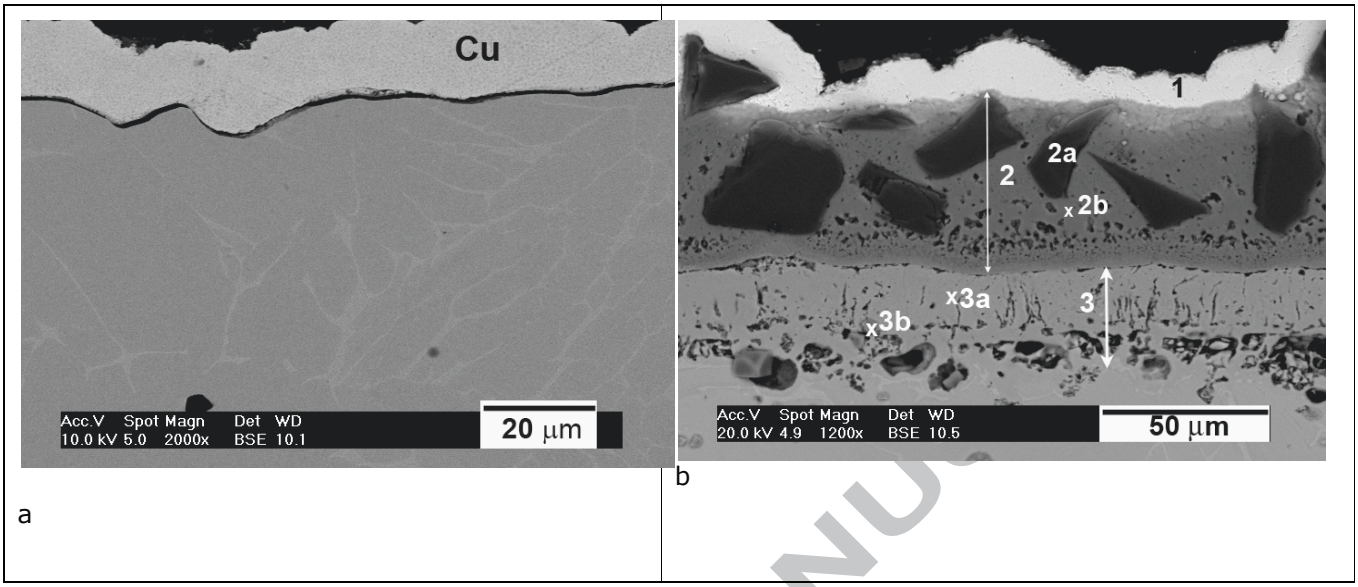

Figure 2. Backscattered electron image of cross section of Ti6Al4V powder metallurgy sample after thermochemical treatment for 2h with NH_4Cl at temperatures of a) 200°C and b) 950°C.

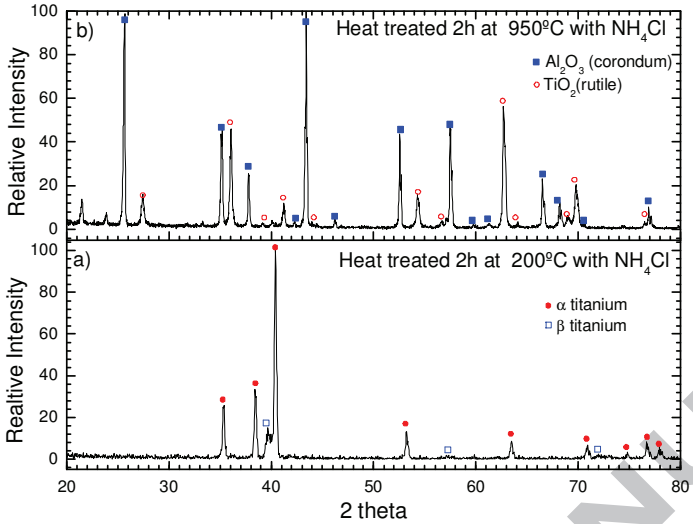

Figure 3. X-ray diffraction patterns of Ti6Al4V powder metallurgy after thermochemical treatment for 2h with NH_4Cl at temperatures of a) 200°C and b) 950°C

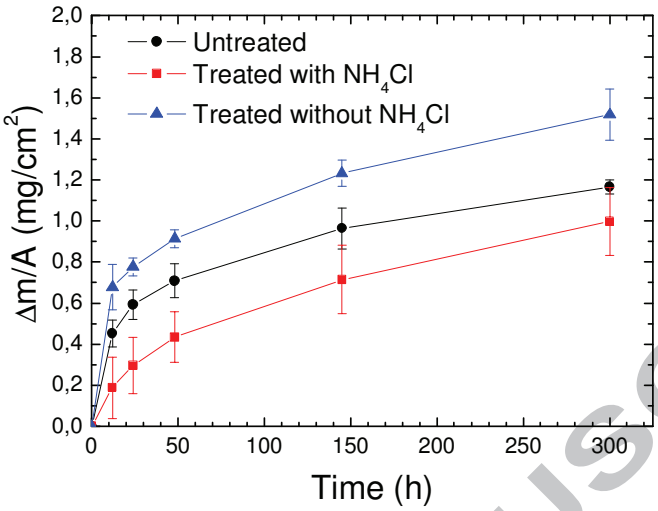

Figure 4. Mass gain with respect to the exposure time in oxidation tests at 600 ºC of powder metallurgy samples treated with and without NH_4Cl at 200ºC for 2h compared to untreated Ti6Al4V PM samples.

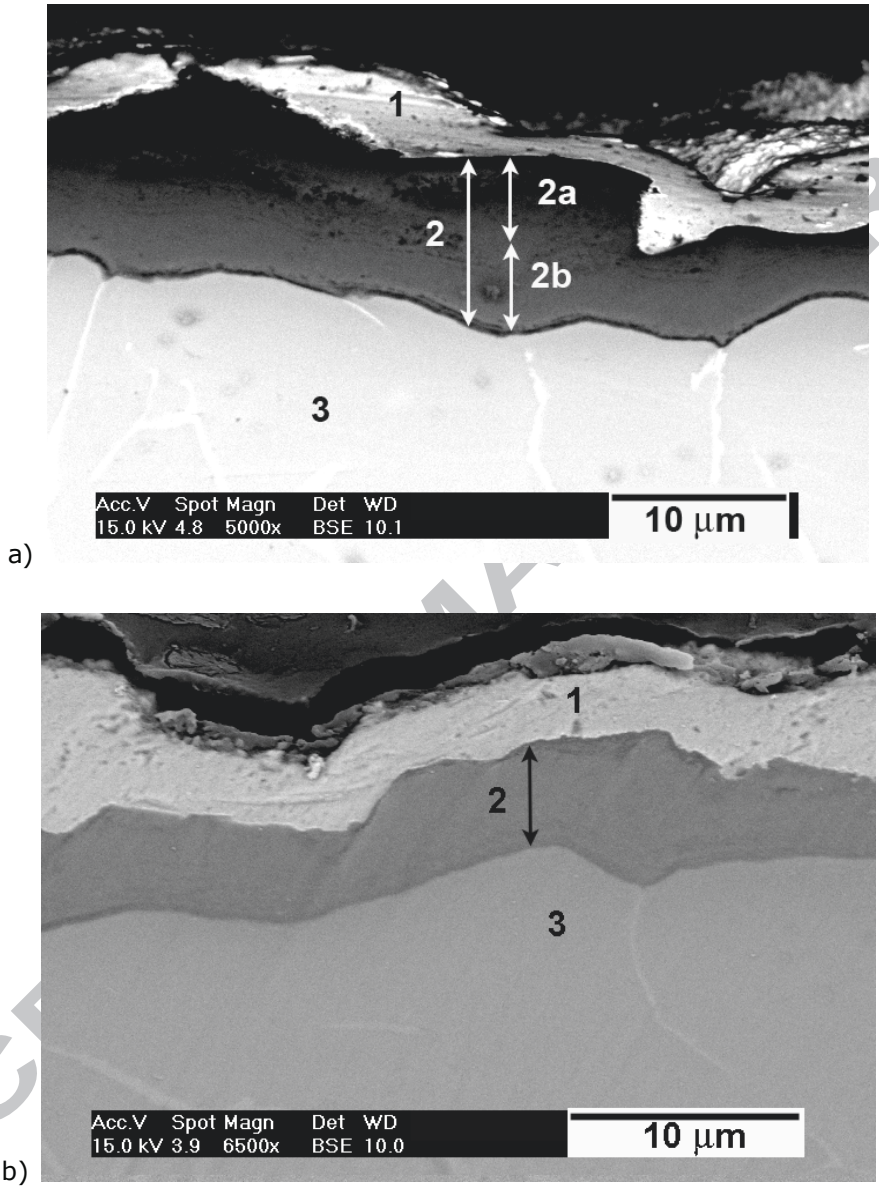

Figure 5. Backscattered electron image of cross section of Ti6Al4V powder metallurgy sample treated for 2h at temperature of 200°C a) with NH_4Cl, b) without NH_4Cl, after oxidation for 300h at 600ºC in air.

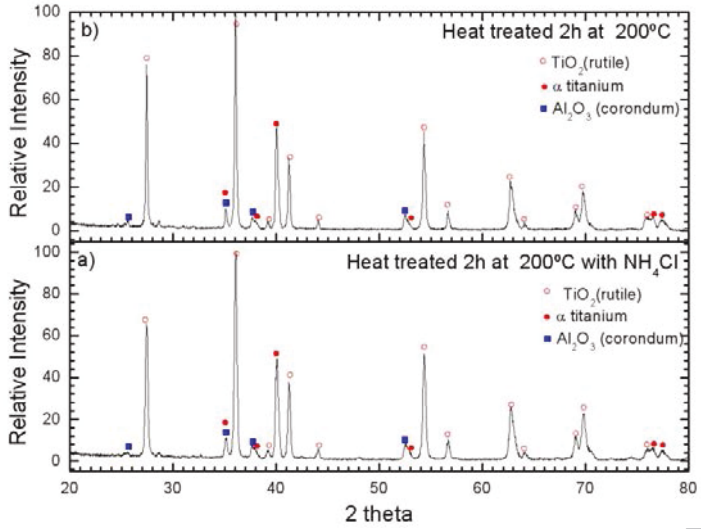

Figure 6. X-ray diffraction patterns of Ti6Al4V powder metallurgy samples treated for 2h at temperature of 200ºC a) with NH_4Cl b) without NH_4Cl, after oxidation for 300 h at 600ºC in air.

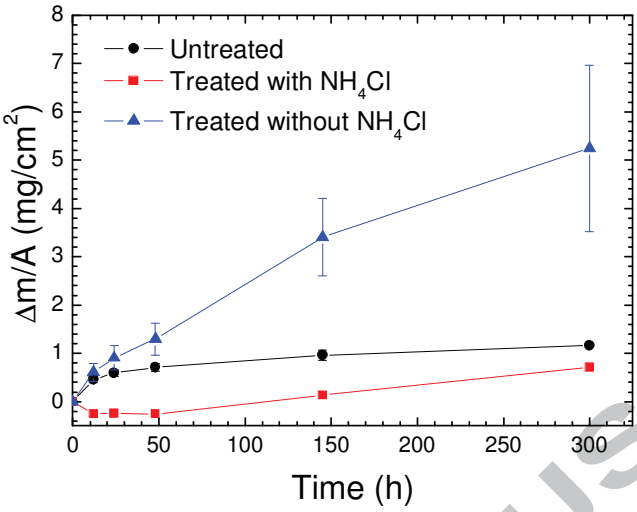

Figure 7. Mass gain with respect to the exposure time in oxidation tests at 600ºC of powder metallurgy samples treated with and without NH_4Cl at 200ºC compared to untreated Ti6Al4V PM samples

a)

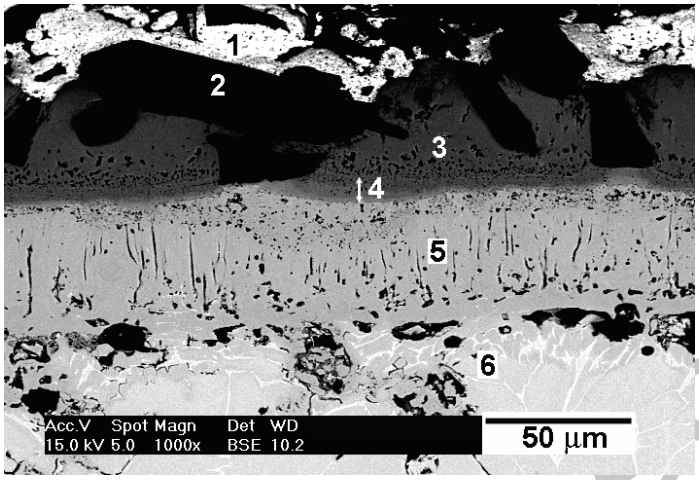

b)

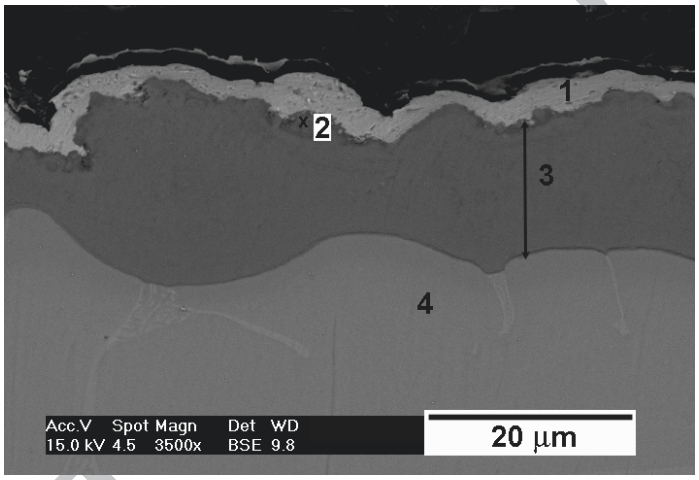

Figure 8. Backscattered electron image of cross section of Ti6Al4V powder metallurgy sample treated for 2h at temperature of 950°C a)with NH_4Cl and b) without NH_4Cl ,after oxidation for 300h at 600ºC in air.

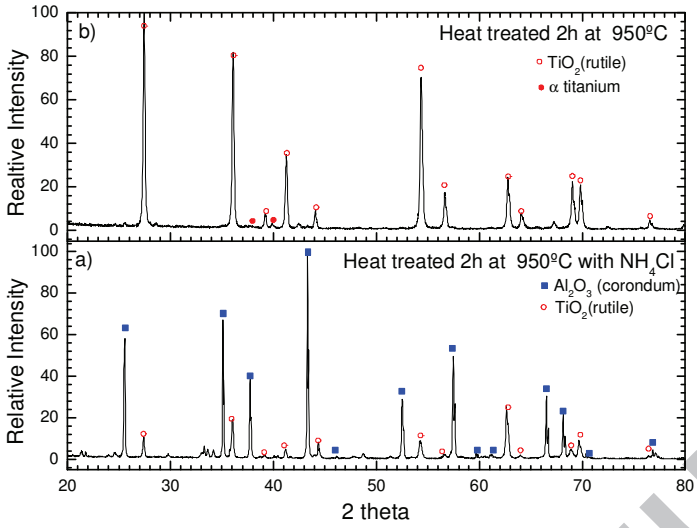

Figure 9. X-ray diffraction patterns of Ti6Al4V powder metallurgy samples treated for 2h at temperature of 950ºC a) with NH_4Cl b) without NH_4Cl, after oxidation for 300 h at 600ºC in air.

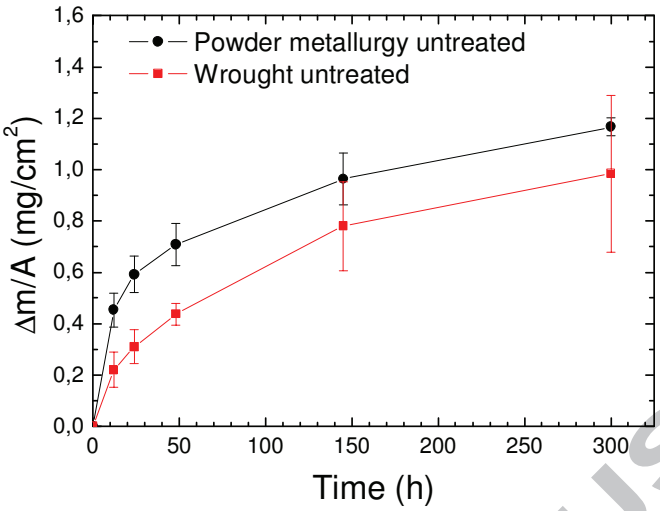

Figure 10. Mass gain with respect to the exposure time in oxidation tests at 600ºC of powder metallurgy Ti6Al4V untreated samples compared to wrought untreated Ti6Al4V samples

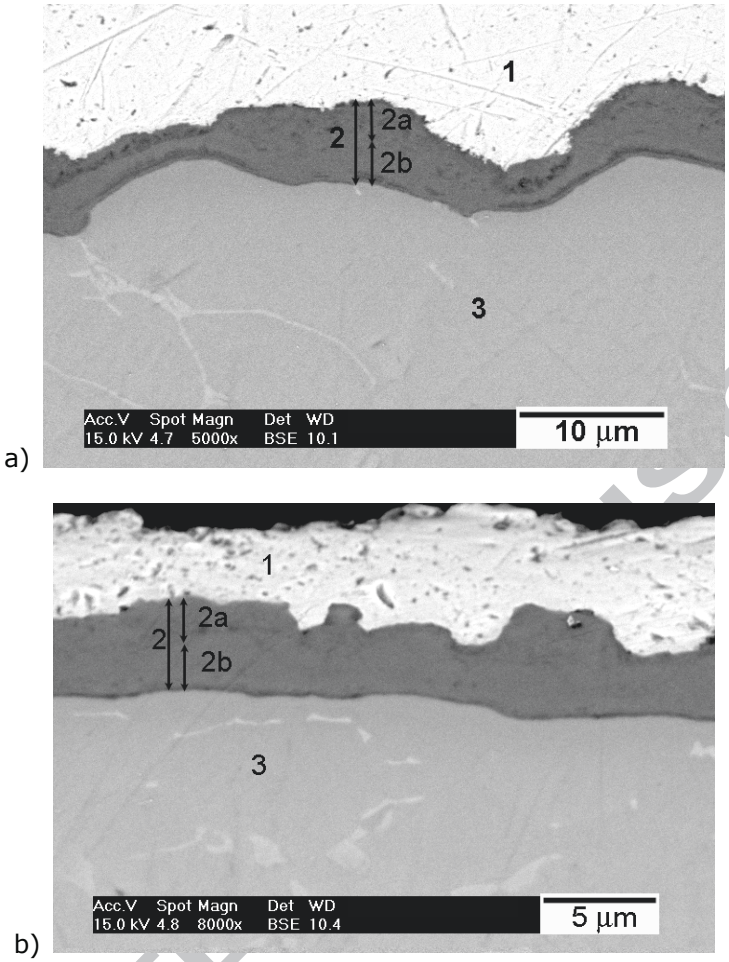

Figure 11a. Backscattered electron image of cross section of Ti6Al4V a) powder metallurgy and b) wrought untreated sample after oxidation for 300h at 600ºC in air

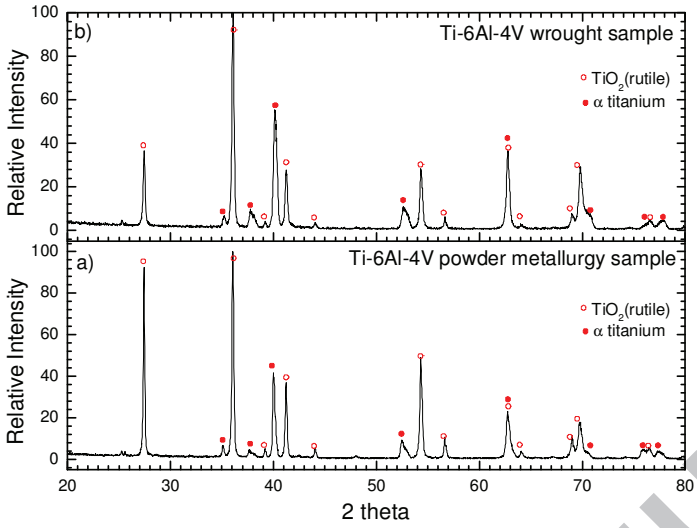

Figure 12. X-ray diffraction patterns of a) powder metallurgy and b) wrought Ti6Al4V samples, after 300 h at 600ºC in air.

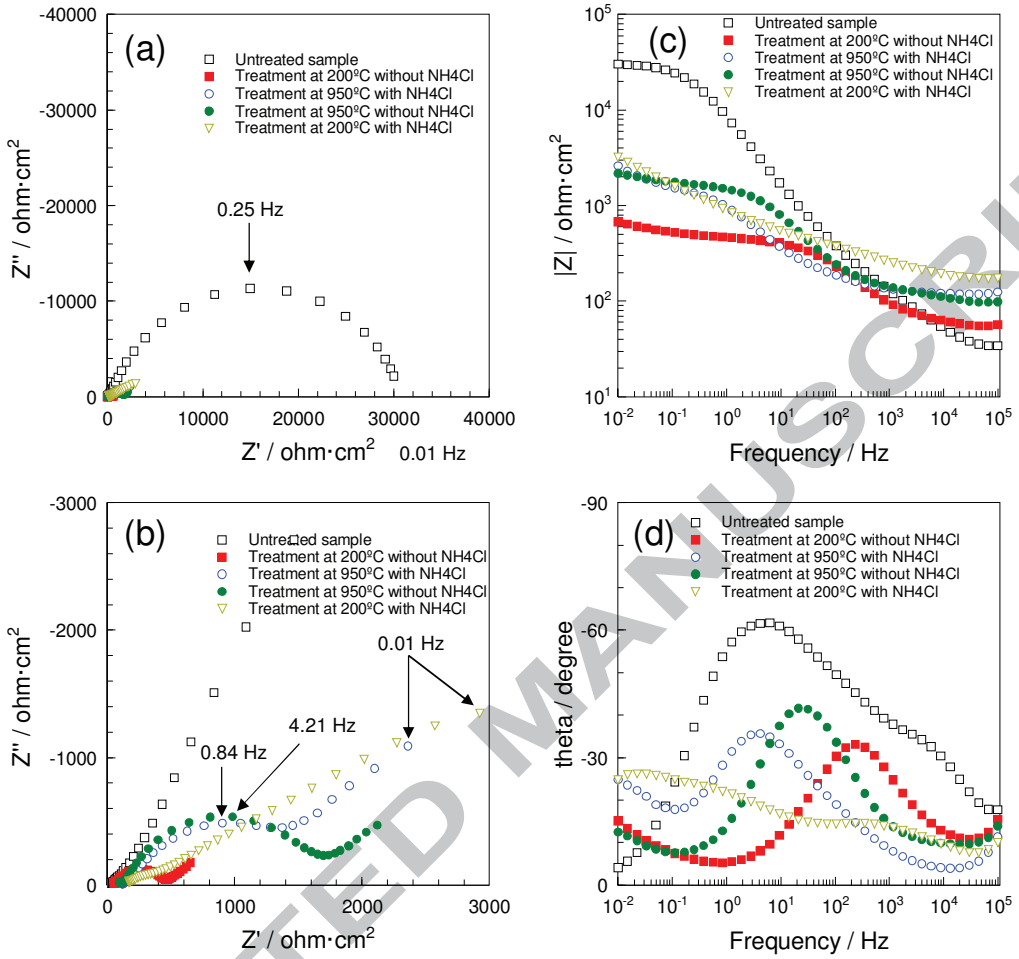

Figure 13. Nyquist and Bode plots for untreated and treated PM Ti6Al4V samples after 5 hours of immersion in Harrison dilute solution: a) Nyquist plot; b)detail of Nyquist plot; c) Bode plot of |Z| versus frequency; d) Bode plot of θ versus frequency. Frequency range applied: 10^5 Hz to 10^{-2} Hz.

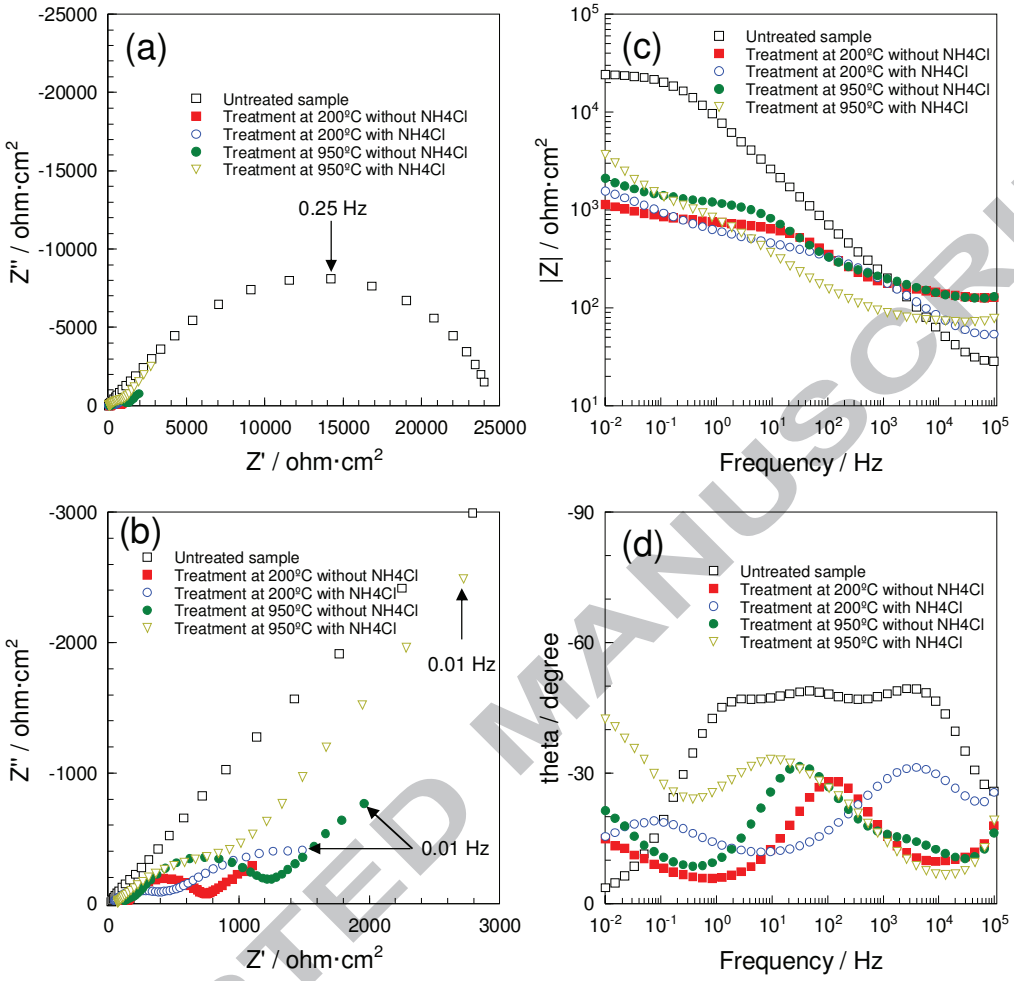

Figure 14. Nyquist and Bode diagrams of untreated and treated PM Ti6Al4V samples after 4 days of immersion in Harrison dilute solution: a) Nyquist plot; b)detail of Nyquist plot; c) Bode plot of |Z| versus frequency; d) Bode plot of θ versus frequency. Frequency range applied:10^{5} Hz to 10^{-2} Hz.

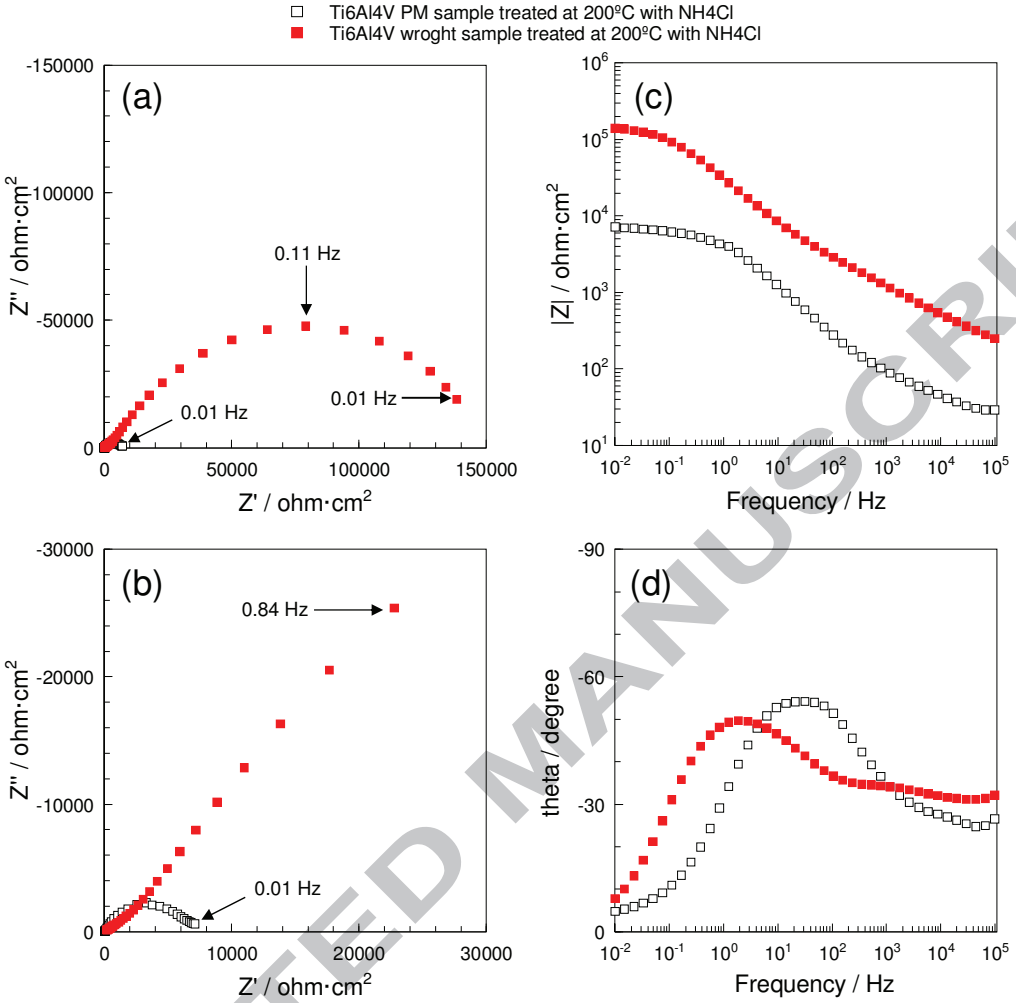

Fig. 15. Nyquist and Bode diagrams obtained for heat-treated wrought and PM Ti6Al4V samples at 200ºC with NH_4Cl, after 4 days of immersion in Harrison dilute solution: a) Nyquist plot; b)detail of Nyquist plot; c) Bode plot of |Z| versus frequency; d) Bode plot of θ versus frequency. Frequency range applied: 10^5 Hz to 10^{-2} Hz. . OCPs: +34 mV for PM Ti6Al4V and +27 mV for Wrought Ti6Al4V (vs Ag/AgCl Ref. electrode), respectively.

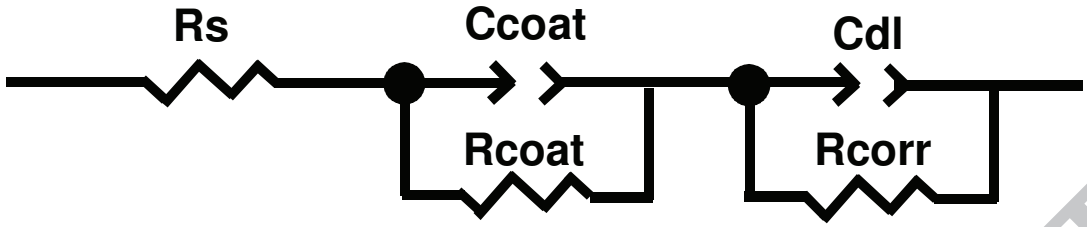

Fig.16 Equivalent circuit proposed for adjustment of impedance behavior

Highlights

- Simple halide treatment with NH_4Cl was carried out on Ti6Al4V alloy
- High temperature oxidation and electrochemical corrosion were evaluated
- Improvement in high temperature oxidation resistance was observed
- Improvement in corrosion resistance was observed for samples treated at 200°C